^{79}Br and ^{127}I NQR of tert-Butylammonium Halides and Crystal Structure of $(CH_3)_3CNH_3^{\oplus}Br^{\ominus}$ *

Morteza Shabazi, Shi-qi Dou, and Alarich Weiss
Institut für Physikalische Chemie, Physikalische Chemie III, Technische Hochschule Darmstadt, Darmstadt, Germany

Z. Naturforsch. **47a,** 171–176 (1992); received June 25, 1991

The ^{79}Br and the ^{127}I NQR spectrum of tert-butylammonium bromide and iodide, respectively, was studied as a function of temperature. No phase transition was observed for the bromide in the temperature range covered. The ^{79}Br NQR frequency is 9.056 MHz at 113 K and increases with increasing temperature (10.040 MHz at 293 K).

The ^{127}I NQR spectrum reveals a phase transition of $(CH_3)_3CNH_3^{\oplus}I^{\ominus}$ around 360 K with pronounced hysteresis. The nuclear quadrupole coupling constant of ^{127}I is 69.335 MHz with an asymmetry parameter of 0.154 for the high temperature phase at $T = 370$ K. For the low temperature phase the corresponding values are 67.136 MHz and 0.081 at 300 K.

The crystal structure of tert-butylammonium bromide was studied at room temperature. The compound crystallizes orthorhombic, space group D_{2h}^{15}-Pbca, with 4 formula units in the unit cell, $a = 1832.1$ pm, $b = 918.5$ pm, $c = 899.8$ pm. The crystal structure and hydrogen bond system are discussed in connection with the NQR results.

Introduction

The tert-butylammonium ion $[(CH_3)_3C(NH_3)]^{\oplus}$ is, in first approximation, nearly spherical; it is an isoelectronic isomer to the tetramethylammonium ion. In tert-butylammonium halides hydrogen bonds are expected and therefore less symmetric crystal structures as those observed for the tetramethylammonium halides are quite likely. In recent time we have studied a number of alkyl- and arylammonium halides by ^{79,81}Br and ^{127}I nuclear quadrupole resonance, NQR, and also by X-ray crystallography. The NQR studies are quite useful to gain a first inside into the symmetry of the solid considered; also phase transitions can be observed in a rather convenient way, see e.g. [1–3]. Furthermore, from the measured frequencies, conclusions about the bond character are possible. In the following we report on ^{79}Br NQR studies of $[(CH_3)_2CNH_3]^{\oplus}Br^{\ominus}$ and on ^{127}I NQR investigations of $[(CH_3)_3CNH_3]^{\oplus}I^{\ominus}$, both as functions of temperature. The crystal structure of tert-butylammonium bromide is also reported.

Recently Ishida et al. [4] have reported ^{1}H NMR studies on the cation motion in tert-butylammonium chloride and bromide.

Experimental

The title compounds were prepared from tert-butylamine (Aldrich), dissolved in an alcohol-water mixture, and hydrobromic acid, hydroiodic acid, respectively. The solutions were concentrated, the precipitated solids separated and recrystallized with water as solvent.

The ^{79}Br- and ^{127}I-NQR measurements have been done with a superregenerative spectrometer. The wanted temperatures of the probes were created by a temperature and flow regulated nitrogen gas stream. The temperatures given are accurate to ± 0.5 K and the frequencies reported are accurate to ± 3 KHz.

For the crystal structure determination a 4-circle diffractometer was used. Suitable crystals for the X-ray work were grown from aqueous solution. The experimental conditions for the X-ray work and some crystallographic data are given in Table 1. The structure was determined by direct methods [5]. The hydrogen coordinates have been taken from difference Fourier synthesis and all coordinates were refined by least squares procedure [6].

---

* Presented at the XIth International Symposium on Nuclear Quadrupole Resonance Spectroscopy, London, United Kingdom, July 15–19, 1991.

Reprint requests to Prof. Dr. Al. Weiss, Institut für Physikalische Chemie, Technische Hochschule Darmstadt, Petersenstraße 20, W-6100 Darmstadt, FRG.

0932-0784 / 92 / 0100-0171 $ 01.30/0. – Please order a reprint rather than making your own copy.

Table 1. Crystal structure of tert-butylammonium bromide $(CH_3)_3CNH_3^{\oplus}Br^{\ominus}$; experimental conditions for the structure determination and crystal structure data.

Formula	$C_4H_{12}BrN$; $M = 154.06$
Crystal habitus	colorless prism $(0.15 \times 0.22 \times 0.35)$ mm^3
Diffractometer	Stoe-Stadi 4
Wavelength λ/pm	71.069 (MoKα)
Monochromator	Graphite (002)
Scan	$\omega/2\theta$
Absorption coefficient/m^{-1}	5208
$F(000)$	642.00
$(\sin \vartheta/\lambda)_{max}$/pm^{-1}	0.005385
Number of reflexions measured	1309
Independent reflexions	983
Reflexions considered	840
Number of free parameters	68
$R(F)$	0.056
$R_w(F)$	0.047
Lattice constants a/pm	1832.1(6)
b/pm	918.5(3)
c/pm	899.8(3)
Volume · 10^{-6}/(pm)^3	1514.16(150)
Space group	D_{2h}^{15}-Pbca
Formula units per unit cell	$Z = 8$
ϱ_c/Mg · m^{-3}	1.35(0)

Point positions: all atoms in 8c:

x, y, z; $\frac{1}{2}+x, \frac{1}{2}-y, \bar{z}$; $\bar{x}, \frac{1}{2}+y, \frac{1}{2}-z$; $\frac{1}{2}-x, \bar{y}, \frac{1}{2}+z$;
$\bar{x}, \bar{y}, \bar{z}$; $\frac{1}{2}-x, \frac{1}{2}+y, z$; $x, \frac{1}{2}-y, \frac{1}{2}+z$; $\frac{1}{2}+x, y, \frac{1}{2}-z$

Results and Discussion

Crystal Structure of tert-Butylammonium bromide

The crystal structure of tert-butylammonium bromide was determined in the usual way (see above). In Table 1 the information on the experimental details is given together with some crystal structure data (lattice constants, space group, etc.). In Table 2 the relative atomic coordinates are listed together with the thermal parameters, and in Table 3 intra- and intermolecular distances are collected. In Fig. 1 the unit cell of the title compound is projected along [010] onto the *ac*-plane. As seen from that projection, each of the three hydrogen atoms of the NH_3 group forms a hydrogen bond with an adjacent $Br^{\ominus}$ ion and each of the bromines in the lattice is involved in three hydrogen bonds, in total a rather simple hydrogen bond scheme. The involved distances Br ... N are between 332 pm and 335 pm, the involved distances –H ··· Br are between 225 pm and 230 pm, see Table 3.

Through the hydrogen bonds, a double chain of ion pairs $[(CH_3)_3CNH_3]^{\oplus}Br^{\ominus}$ is formed, running along [001] at $x = 0.25$ and at $x = 0.75$. The planes (100) and (200) are the ones through which van der Waals interactions of CH_3 groups should exist; solid tert-butylammonium bromide forms a layer lattice. Ishida et al. [4] determined from powder diffraction data the unit cell of tert-butylammonium bromide to be orthorhombic; the lattice constants they give (1831 pm, 918 pm, and 900 pm) are in very good agreement with the results from the present single crystal study. These authors also state that tert-butylammonium chloride is isomorphous with tert-butylammonium bromide.

^{79}Br NQR Spectrum of tert-Butylammonium bromide

In Fig. 2 we show the temperature dependence of the ^{79}Br spectrum of $(CH_3)_3CNH_3Br$. We have parameterized $\nu(^{79}Br) = f(T)$ according to

$$\nu = \sum_{i=-1}^{2} a_i T^i. \tag{1}$$

In Table 4 the coefficients of (1) are listed for the ^{79}Br NQR spectrum in $(CH_3)_3CNH_3^{\oplus}Br^{\ominus}$. The ^{79}Br NQR

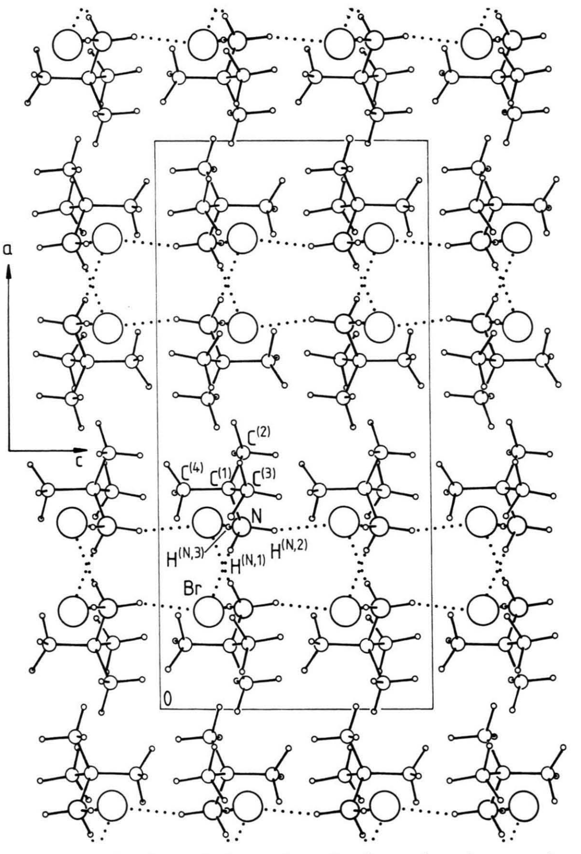

Fig. 1. Projection of the unit cell of tert-butylammonium bromide, $(CH_3)_3CNH_3^{\oplus}Br^{\ominus}$, along [010] onto the *ac*-plane. The ions marked by * are the ones for which the coordinates are given in Table 2.

Table 2. Positional and thermal parameters of tert-butylammonium bromide $(CH_3)_3CNH_3^{\oplus}Br^{\ominus}$; the temperature factor is of the form:

$$T=\exp[-2\pi^2(U_{11}h^2a^{*2}+U_{22}k^2b^{*2}+U_{33}l^2c^{*2}+2U_{12}hka^*b^*+2U_{13}hla^*c^*+2U_{23}klb^*c^*)]\,.$$

The U_{ij} are given in (pm)^2; U is isotropic mean for the hydrogen atoms.

Atom	x/a	b/y	z/c	$U_{11}(U)$	U_{22}	U_{33}	U_{12}	U_{13}	U_{23}
Br	0.1713(1)	0.0816(1)	0.1812(1)	759(7)	763(7)	602(6)	118(6)	−83(6)	−44(6)
N	0.3222(3)	−0.0793(7)	0.3095(6)	452(42)	629(43)	531(38)	29(37)	10(37)	55(41)
$C^{(1)}$	0.3880(5)	0.0045(11)	0.2587(11)	573(67)	866(70)	792(67)	−134(58)	99(61)	4(64)
$C^{(2)}$	0.4526(5)	−0.0814(11)	0.3162(11)	586(66)	1153(88)	1149(87)	−148(65)	106(68)	−247(87)
$C^{(3)}$	0.3839(6)	0.1552(9)	0.3271(13)	1063(86)	746(45)	1318(95)	−335(65)	242(81)	−115(82)
$C^{(4)}$	0.3864(6)	0.0093(13)	0.0922(9)	1033(93)	1518(107)	654(66)	−278(80)	246(71)	194(79)
$H'(N)$	0.2798(3)	−0.0116(7)	0.2631(6)	600					
$H''(N)$	0.3135(3)	−0.0915(7)	0.4276(6)	600					
$H'''(N)$	0.3209(3)	−0.1851(7)	0.2571(6)	600					
$H'(C^{(2)})$	0.5039(5)	−0.0360(11)	0.2795(11)	600					
$H''(C^{(2)})$	0.4503(5)	−0.1953(11)	0.2868(11)	600					
$H'''(C^{(2)})$	0.4480(5)	−0.0702(11)	0.4353(11)	600					
$H'(C^{(3)})$	0.4356(6)	0.2087(9)	0.3080(13)	600					
$H''(C^{(3)})$	0.3708(6)	0.1596(9)	0.4440(13)	600					
$H'''(C^{(3)})$	0.3417(6)	0.2096(9)	0.2643(13)	600					
$H'(C^{(4)})$	0.4305(6)	0.0592(13)	0.0308(9)	600					
$H''(C^{(4)})$	0.3360(6)	0.0655(13)	0.0680(9)	600					
$H'''(C^{(4)})$	0.3815(6)	−0.1036(13)	0.0602(9)	600					

Table 3. Crystal structure of tert-butylammonium bromide $(CH_3)_3CNH_3^{\oplus}Br^{\ominus}$. Intra- and interionic distances, d/pm, and angles (°).

Atoms *	d/pm	Atoms	Angles/°
$C^{(1)}-N$	150.1(10)	$N-C^{(1)}-C^{(2)}$	104.8(8)
$C^{(1)}-C^{(2)}$	151.3(12)	$N-C^{(1)}-C^{(3)}$	107.8(8)
$C^{(1)}-C^{(3)}$	151.7(12)	$N-C^{(1)}-C^{(4)}$	107.7(8)
$C^{(1)}-C^{(4)}$	149.9(11)	$C^{(2)}-C^{(1)}-C^{(3)}$	112.1(9)
		$C^{(2)}-C^{(1)}-C^{(4)}$	111.9(10)
$Br' \ldots N$	334.2(6)	$C^{(3)}-C^{(1)}-C^{(4)}$	112.2(10)
$Br'' \ldots N$	334.6(6)		
$Br''' \ldots N$	332.3(6)	$Br' \ldots H'(N)-N$	165.2(1)
$Br' \ldots H'(N)$	228.6(6)	$Br'' \ldots H''(N)-N$	162.5(1)
$Br'' \ldots H''(N)$	230.0(6)	$Br''' \ldots H'''(N)-N$	170.7(1)
$Br''' \ldots H'''(N)$	225.3(6)		
$C^{(2)} \ldots C'^{(2)}$	402.5(12)		
$C^{(2)} \ldots C'^{(3)}$	406.0(12)		
$C^{(3)} \ldots C'^{(4)}$	389.7(12)		

* Br':	0.1713	0.0816	0.1812
Br'':	0.3287	−0.0816	0.6812
Br''':	0.3287	−0.4184	0.1812
$C'^{(2)}$:	0.5474	0.0814	0.6838
$C'^{(3)}$:	0.6161	−0.3448	0.1729
$C'^{(4)}$:	0.3864	0.4907	0.5922

spectrum consists of a single line, in agreement with the crystal structure determination which revealed only one crystallographically independent bromine ion in the unit cell. (The ^{81}Br NQR frequency at ambient temperatures was registered, too, for completeness.) Furthermore, $\nu(^{79}Br)=f(T)$ is a smooth curve; no phase transition is indicated. $\nu(^{79}Br)$ decreases with decreasing temperature, an unusual behavior, not expected from the Bayer theory [7, 8] of the temperature dependence of NQR frequencies. Most likely, the dynamical behavior of the cation in the lattice may be responsible for the positive temperature coefficient found. Also, the rather low mean NQR frequency points to a mainly ionic situation of the bromine ions in the lattice; in such cases the theory of Bayer is not adequate. We have anions $Br^{\ominus}$ in the lattice, and the electric field gradient tensor, EFGT, at the $Br^{\ominus}$ site is determined by the ion distribution in the lattice and by the hydrogen bonds $N-H \cdots Br$. The latter effect could be studied by changing the hydrogen bond strength to a certain extent via a replacement of H by D. From the ^{79}Br NQR frequencies, which are rather low, a small EFG must exist at the bromine site. This is not surprising, since the three hydrogen bonds to the $Br^{\ominus}$ are of quite symmetric geometry, with nearly equal distances and nearly equal angles $N-H \cdots Br$, see Table 3 and Figure 1. We could not observe the ^{79}Br NQR below 100 K; no signal was observed at 77 K. This disappearance of the ^{79}Br NQR may well be connected with a phase transition at around 100 K due to some change in the dynamical behavior of either the NH_3 group or the CH_3 groups or both.

From their T_1 (^{1}H)-MNR measurements, Ishida et al. [4] have been able to calculate the activation energy of the cation motion in tert-butylammonium bromide

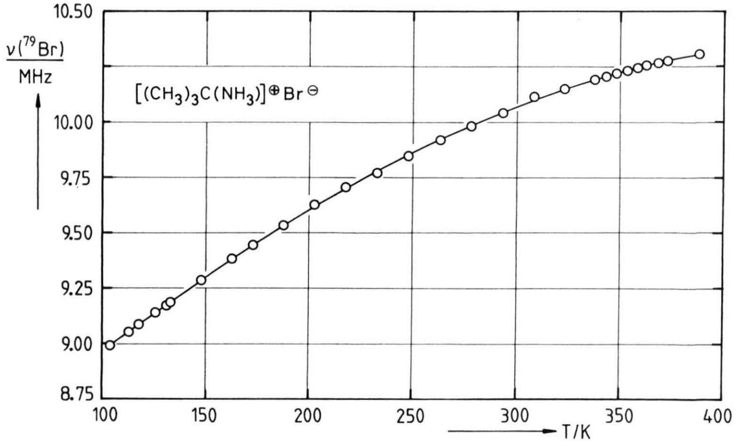

Fig. 2. ^{79}Br NQR frequency of tert-butylammonium bromide, $(CH_3)_3CNH_3^{\oplus}Br^{\ominus}$, as a function of temperature.

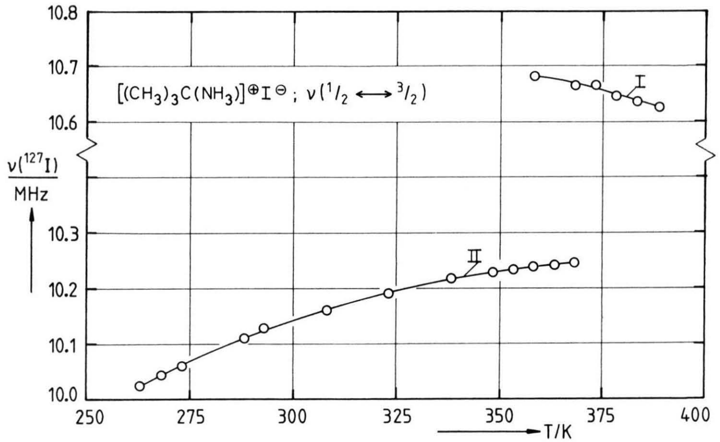

Fig. 3. $\nu_1(^{127}I)$, $m=\pm 1/2 \leftrightarrow m=\pm 3/2$, of $(CH_3)_3CNH_3^{\oplus}I^{\ominus}$ as a function of temperature.

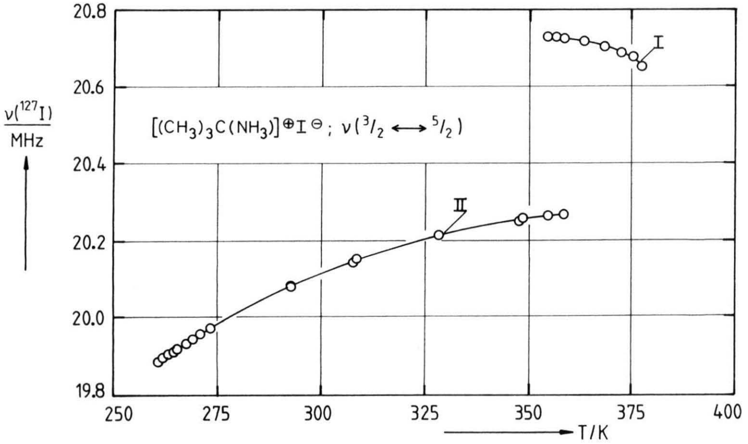

Fig. 4. $\nu_2(^{127}I)$, $m=\pm 3/2 \leftrightarrow m=\pm 5/2$, of $(CH_3)_3CNH_3^{\oplus}I^{\ominus}$ as a function of temperature.

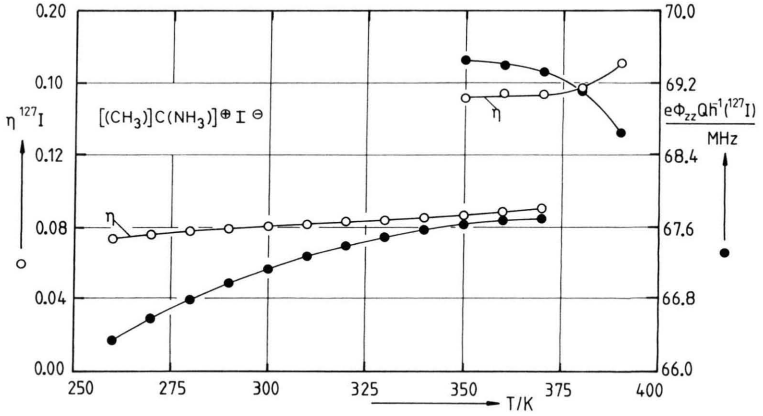

Fig. 5. Nuclear quadrupole coupling constant $e\Phi_{zz}Qh^{-1}$ (^{127}I) and asymmetry parameter $\eta(^{127}I)$ of $(CH_3)_3CNH_3^{\oplus}I^{\ominus}$ as a function of temperature.

Table 4. Temperature dependence of $\nu(^{79}\mathrm{Br})$ in $(\mathrm{CH_3})_3\mathrm{CNH}_3^{\oplus}\mathrm{I}^{\ominus}$ and of $\nu(^{127}\mathrm{I})$ in $(\mathrm{CH_3})_3\mathrm{CNH}_3^{\oplus}\mathrm{I}^{\ominus}$: $\nu = a_{-1}T^{-1} + a_0 + a_1 T + a_2 T^2$. Also some resonance frequencies are given for selected temperatures. n is the number of data point taken in the experiments and σ is the standard deviation in the least squares adjustment. $T_1 \ldots T_2$ is the temperature range for which the polynomial is valid.

I. $(\mathrm{CH_3})_3\mathrm{CNH_3Br}$

	n	$\sigma \cdot 10^3$ / MHz	a_{-1} / MHz · K	a_0 / MHz	$a_1 \cdot 10^2$ / MHz · K^{-1}	$a_2 \cdot 10^5$ / MHz · K^{-2}	$T_1 \ldots T_2$ / K
^{79}Br	28	5	17.117998	7.85159	1.057	−1.11229	104−388

$\nu(^{79}\mathrm{Br}) = 9.056$ MHz (113.0 K); $\nu(^{79}\mathrm{Br}) = 10.040$ MHz ($T = 293.5$ K).

II. $(\mathrm{CH_3})_3\mathrm{CNH_3I}$

a) High temperature phase (Phase I)

1. $\nu_1(^{127}\mathrm{I})$, transition $m = \pm 1/2 \leftrightarrow m = \pm 3/2$

	n	$\sigma \cdot 10^3$ / MHz	a_{-1} / MHz · K	a_0 / MHz	$a_1 \cdot 10^2$ / MHz · K^{-1}	$a_2 \cdot 10^5$ / MHz · K^{-2}	$T_1 \ldots T_2$ / K
$\nu_1(^{127}\mathrm{I})$	6	6	−21850.463	183.782	−45.50335	39.6651	358−389

$\nu_1(^{127}\mathrm{I}) = 10.682$ MHz ($T = 358.3$ K); $\nu_1(^{127}\mathrm{I}) = 10.626$ MHz ($T = 388.8$ K).

2. $\nu_2(^{127}\mathrm{I})$, transition $m = \pm 3/2 \leftrightarrow m = \pm 5/2$

	n	$\sigma \cdot 10^3$ / MHz	a_{-1} / MHz · K	a_0 / MHz	$a_1 \cdot 10^2$ / MHz · K^{-1}	$a_2 \cdot 10^5$ / MHz · K^{-2}	$T_1 \ldots T_2$ / K
$\nu_1(^{127}\mathrm{I})$	8	4	142067.283	−1162.775	328.765	−304.543	354−377

$\nu_2(^{127}\mathrm{I}) = 20.730$ MHz ($T = 354.5$ K); $\nu_2(^{127}\mathrm{I}) = 20.654$ MHz ($T = 377.5$ K).

b) Low temperature phase (Phase II)

1. $\nu_1(^{127}\mathrm{I})$, transition $m = \pm 1/2 \leftrightarrow m = \pm 3/2$

	n	$\sigma \cdot 10^3$ / MHz	a_{-1} / MHz · K	a_0 / MHz	$a_1 \cdot 10^5$ / MHz · K^{-1}	$a_2 \cdot 10^8$ / MHz · K^{-2}	$T_1 \ldots T_2$ / K
$\nu_1(^{127}\mathrm{I})$	13	2	−413.1403	11.9690	−90.8000	−197.043	263−368

$\nu_1(^{127}\mathrm{I}) = 10.024$ MHz ($T = 263.1$ K); $\nu_1(^{127}\mathrm{I}) = 10.245$ MHz ($T = 368.3$ K).

2. $\nu_2(^{127}\mathrm{I})$, transition $m = \pm 3/2 \leftrightarrow m = \pm 5/2$

	n	$\sigma \cdot 10^3$ / MHz	a_{-1} / MHz · K	a_0 / MHz	$a_1 \cdot 10^5$ / MHz · K^{-1}	$a_2 \cdot 10^8$ / MHz · K^{-2}	$T_1 \ldots T_2$ / K
$\nu_2(^{127}\mathrm{I})$	20	2	−358.9293	19.4380	1202.9305	−1928.81	261−358

$\nu_2(^{127}\mathrm{I}) = 19.902$ MHz ($T = 263.0$ K); $\nu_2(^{127}\mathrm{I}) = 20.270$ MHz ($T = 358.5$ K).

	T / K	$e\Phi_{zz}Qh^{-1}(^{127}\mathrm{I})$ / MHz	$\eta(^{127}\mathrm{I})$		T / K	$e\Phi_{zz}Qh^{-1}(^{127}\mathrm{I})$ / MHz	$\eta(^{127}\mathrm{I})$
Phase I	350	69.468	0.1521	Phase II	260	66.344	0.0740
	360	69.409	0.1547		280	66.789	0.0781
	370	69.335	0.1540		300	67.136	0.0809
	380	69.122	0.1574		320	67.398	0.0833
	390	68.649	0.1716		340	67.577	0.0854
					350	67.637	0.0870
					360	67.681	0.0887
					370	67.706	0.0908

(and chloride). The activation energy found is fairly high, 38.5 kJ · mol^{-1} and 44.2 kJ · mol^{-1} for the bromide and chloride, respectively. The important role, the hydrogen bonds $NH_3 \cdots Br$ play in hindering the cation motion is supported by the experiments of Ratcliffe and Dunell [9] who investigated tert-butylammonium bromide and chloride with the deuterated group $-ND_3^{\oplus}$. Here, the activation energy for the reorientation of the group $-C(CH_3)_3$ is lower, 32.6 kJ · mol^{-1} for $[(CH_3)_3CND_3]Br$.

^{127}*I NQR on tert-Butylammonium iodide*

In Figs. 3 and 4 the ^{127}I NQR spectrum of $[(CH_3)_3C(NH_3)]^{\oplus}I^{\ominus}$ is shown as a function of temperature. Figure 3 gives the frequencies ν_1 for the transition $m = \pm 1/2 \leftrightarrow m = \pm 3/2$ and in Fig. 4 the frequencies ν_2 for the transition $m = \pm 3/2 \leftrightarrow m = \pm 5/2$ are plotted. In Table 4 we have listed the coefficients of the power series development for $\nu(^{127}I) = f(T)$, following (1). From the frequencies for both transitions, the nuclear quadrupole coupling constant, NQQC, given as $e^2 q Q h^{-1} = e \Phi_{zz} Q h^{-1}$ and the asymmetry parameter $\eta = |\Phi_{xx} - \Phi_{yy}| / |\Phi_{zz}|$ of the EFG can be calculated by solving the secular equation [10]. e is the unit charge, Q the nuclear quadrupole moment, $\Phi_{zz} = eq$ is the main principal axis of the EFGT, and h is the Planck quantum number. Following [9], $e \Phi_{zz} Q h^{-1}$ (^{127}I) and $\eta(^{127}I)$ have been calculated; the results are listed in Table 3 and shown graphically in Figure 5. From Figs. 3–5, on a first glance, one immediately recognizes that there is a phase transition of $[(CH_3)_3C(NH_3)]^{\oplus}I^{\ominus}$ in the temperature range 350 K to 370 K. The transition shows pronounced hysteresis. By increasing the temperature, the low temperature phase II transforms into the high temperature phase I at ≈370 K whereas the transition of phase I into phase II, by lowering the temperature, occurs at ≈350 K. Without information on the crystal structure, at present time, we can draw the following conclusions about the structure from the ^{127}I NQR results [11]:

a) Below 260 K no NQR signal is observable; a freezing in of some degree of freedom of the cation may occur in this temperature range,

b) the temperature dependence of $\nu_1, \nu_2, e\Phi_{zz} Q h^{-1}$ (^{127}I), and $\eta(^{127}I)$ show a strong influence of molecular dynamics on the EFG acting at the iodine site in phase II,

c) both, phase I and phase II have only one crystallographically independent iodine in the unit cell and quite likely one of the two phases observed may be isomorphous to $(CH_3)_3CNH_3Br$.

Acknowledgement

We are grateful to Dr. P. Storck for interesting discussions. M. Shabazi is thankful to the Deutscher Akademischer Austauschdienst (DAAD), for a fellowship. The work was supported by the Bundesminister für Forschung und Technologie (project no. 03WS2DAR9).

[1] A. Kehrer, Shi-qi Dou, and Al. Weiss, Z. Naturforsch. **44a,** 659 (1989).
[2] J. Hartmann, Shi-qi Dou, and Al. Weiss, Z. Naturforsch. **44a,** 41 (1989).
[3] J. Hartmann and Al. Weiss, Ber. Bunsenges. Phys. Chem. **91,** 1195 (1987).
[4] H. Ishida, S. Inada, N., Hayama, D. Nakamura, and R. Ikeda, Z. Naturforsch. **46a,** 256 (1991).
[5] G. M. Sheldrick, Program for Crystal Structure Determination, University of Göttingen, Germany 1986.
[6] G. M. Sheldrick, Program for Crystal Structure Determination, University of Cambridge, England 1976.
[7] H. Bayer, Z. Physik **130,** 227 (1951).
[8] R. J. C. Brown, Z. Naturforsch. **45a,** 449 (1990).
[9] C. I. Ratcliffe and B. A. Dunell, J. Chem. Soc. Faraday Trans. 2, **77,** 2041 (1981).
[10] R. B. Creel, H. R. Brooker, and R. G. Barnes, J. Magn. Reson. **41,** 146 (1980).
[11] Further information on the crystal structure determination may be obtained from Fachinformationszentrum Karlsruhe, Gesellschaft für wissenschaftlich-technische Information mbH, W-7514 Eggenstein-Leopoldshafen 2, Germany. Inquiries should be accompanied by the depository number CSD-55469, the names of the authors, and the full literature reference.